Remarkable Features in the Interactions of Quadrupolar Molecules

ARTICLE *in* THE JOURNAL OF PHYSICAL CHEMISTRY A · APRIL 2006

Impact Factor: 2.69 · DOI: 10.1021/jp0575355 · Source: PubMed

3 AUTHORS, INCLUDING:

Heather Jaeger
Lehigh University
17 PUBLICATIONS **171** CITATIONS

SEE PROFILE

FEATURE ARTICLE

Remarkable Features in the Interactions of Quadrupolar Molecules

Heather M. Jaeger, David W. H. Swenson, and Clifford E. Dykstra*

Department of Chemistry and Chemical Biology, Indiana University−Purdue University Indianapolis, 402 North Blackford Street, Indianapolis, Indiana 46202

Received: December 27, 2005; In Final Form: February 20, 2006

Quadrupolar charge fields of molecules and of molecular fragments give rise to unique features in weakly interacting clusters and aggregations. Relative to dipole−dipole interactions, the interactions among quadrupolar molecules tend to allow for greater orientational distortions away from equilibrium. Potential surface regions have been found for several clusters that are attractive and yet very flat for certain directions. There is a notable slipperiness for the interactions in some of these cases. This implies significant vibrational excursions even in the ground state. Furthermore, the coupling of rotations among nearby molecules in pure clusters of quadrupolar molecules is different than for dipolar species, and it can lead to unexpectedly small internal rotation barriers. How these and other features develop and what they might imply for materials and biomolecular simulations are discussed here.

Introduction

There is a chemistry of weak, noncovalent bonding with patterns for structures and energetics, and it operates alongside the chemistry of covalent and ionic bonding. Within this weak bonding chemistry, one finds dispersion effects between molecules, which are manifested in an overall, long-range attractiveness between atoms of interacting molecules, and one finds electrostatic interactions that often provide a significant orientational influence. For closed-shell neutral species, the strongest electrostatic effect is that of the dipole−dipole interaction. However, many molecules are nonpolar, or more precisely, nondipolar. For most of these, the orientational influence that goes with electrostatic interactions comes about via their quadrupolar charge fields. The nature of the orientational influence in this case, especially when viewed together with all other contributors to weak interaction energies, has features that are remarkable, particularly as more and more quadrupolar molecules interact.

If the story of quadrupolar interactions among molecules has a definite beginning point, it is probably with the work of Buckingham [see, for instance, ref 1]. Quadrupolar molecules are simply those neutral molecules that have a zero permanent dipole moment but a nonzero quadrupole moment. Acetylene, for example, is a quadrupolar molecule with the hydrogens at the ends carrying a partial positive charge balanced by a partial negative charge between. All molecules with an inversion center of symmetry do not have a dipole but may have a sizable quadrupole.

To talk about interactions involving quadrupolar molecules, it is best to consider quadrupole charge fields of molecules as opposed to ideal or point quadrupoles. Benzene is an example. Above and below the plane of the benzene ring are identical electron π-clouds. Their negative charge density is balanced by a positive charge density in the plane of the molecule where the nuclei are, and in that, the molecule can be identified as a quadrupolar species. However, an ideal (point) quadrupole at the center of benzene with the same moment (tensor elements) as that of benzene would generate a field exactly like that of benzene only in the long-range limit. Close-in, the charge field requires either higher order multipoles or a distribution of point multipoles that reflects the molecule's spatial extent. The molecules considered herein as quadrupolar species are those with a quadrupole as their lowest-order nonvanishing electrical moment, without presuming that a point quadrupole necessarily represents the true charge field of the species.

Many quadrupolar molecules of interest have hydrogen atoms, and that fact connects the topic of this report with hydrogen bonding, something ubiquitous and significant throughout the chemical sciences. Although elementary concepts related to hydrogen bonding often invoke the role of interacting dipoles, sometimes reduced to that of positive and negative point charges, quadrupolar species are not precluded from exhibiting hydrogen bonding. In fact, a local H−C dipole exists in a quadrupolar molecule such as ethylene and contributes to the molecule's weak, hydrogen bonding with other species. Of interest is how the other H−C dipoles act together to influence orientational features. A local dipole interaction picture on its own (only the proximate local dipole interacting with a partner) is insufficient at giving the features we are coming to recognize as common to the interactions among quadrupolar species.

Modeling the Interaction Potentials of Quadrupolar Species

A model potential is very valuable for the investigation of clusters with interacting quadrupolar molecules, particularly clusters with many molecules and therefore many geometrical degrees of freedom. Studying progressively larger clusters provides information on aggregation, especially how attachment energies evolve with cluster size. Ab initio calculations can, and for our interests do, reach a size limit that does not provide

10.1021/jp0575355 CCC: $33.50
Published on Web 04/25/2006

Heather M. Jaeger will receive a B.S. in Chemistry in 2006 from Indiana University−Purdue University Indianapolis. She started as a freshman at IUPUI in 2003 and developed an interest in computational research about the time she took several advanced chemistry courses. She has been working in Dykstra's research group for nearly a year.

David W. H. Swenson received a B.A. from Colorado College (Colorado Springs, CO) in 2003, simultaneously completing majors in Chemistry, French Literature, and Physics. He spent three summers at Indianapolis carrying out computational work in Dykstra's research group. He also earned an undergraduate degree in Mathematics from Université Louis Pasteur (Strasbourg, France) in 2005. He is currently pursuing a Ph.D. at the University of California, Berkeley, working under the direction of Professor William H. Miller.

Clifford E. Dykstra received B.S. degrees in Chemistry and in Physics in 1973 from the University of Illinois at Urbana-Champaign and received his Ph.D. from the University of California at Berkeley in 1976. He joined the faculty of the University of Illinois at Urbana-Champaign in 1977 and moved to Indiana University−Purdue University Indianapolis in 1990 where he is Chancellor's Professor in the Department of Chemistry and Chemical Biology. His research interests began with methods development in ab initio electronic structure theory, including methods for the calculational investigation of electrical and magnetic properties of molecules. That, in turn, sparked his interests in the relationship between molecular properties and intermolecular interaction phenomena.

all the answers. On the other hand, a model potential, subject to its accuracy, can be used for much, much larger clusters than those for which ab initio calculations can be performed. In addition, evaluating zero point energies (ZPE), which are important for having the most complete stability information, is aided by a model potential. The weak, intermolecular vibrational modes of clusters tend to be very anharmonic, and harmonic estimates of zero point energies for H_2 clusters, for instance, overshoot the true ZPE by much more than the well depth.[2] Fully anharmonic ZPE values can be obtained from detailed vibrational analysis, but typically, this requires repeated evaluations of the interaction energy. Again, a concise and reliable model potential is advantageous.

The model potential we have used for clusters with quadrupolar species follows the form of the molecular mechanics for clusters (MMC) scheme[3] because the MMC form means the potential can be immediately applied to larger clusters. With this scheme, the interaction energy, V, is developed for rigid monomers and is a function of the spatial coordinates of the molecular centers of mass and the orientation angles about the centers of mass. We use a set of Euler angles to specify orientations. The interaction energy is expressed as a sum of the classically evaluated electrical interaction energy, $V_{\text{electrical}}$, plus a term, $V_{\text{nonelectrical}}$, involving Lennard-Jones or 6-12 terms among different monomer sites. These sites are mostly the positions of the atomic nuclei. The electrical interaction ($V_{\text{electrical}}$) is the sum of the permanent moment interaction and polarization energy based on electrical response properties of the monomers. The nonelectrical interaction ($V_{\text{nonelectrical}}$) uses a small number of adjustable parameters.

$$V = V_{\text{electrical}} + V_{\text{nonelectrical}} \tag{1}$$

$$V_{\text{nonelectrical}} = \sum_{\text{A,B>A}}^{\text{molecules}} V_{\text{AB}} \tag{2}$$

$$V_{\text{AB}} = \sum_{\alpha=1}^{\text{A sites}} \sum_{\beta=1}^{\text{B sites}} \left(\frac{d_\alpha d_\beta}{r_\alpha \beta^{12}} - \frac{c_\alpha c_\beta}{r_\alpha \beta^{6}} \right) \tag{3}$$

Equation 3 shows that the adjustable parameters, designated c and d, enter the nonelectrical part of the model potential as products. Note that the c and d parameters are always taken to be positive or zero. The use of products of coefficients in the 6-12 terms in eq 3 means that parameters are associated with individual molecules, not with interacting pairs of molecules. This implies, or one might say enforces, transferability in that parameters obtained for some molecule A are taken to be good for use in A−B interactions, A−C interactions and so on. This also means that the number of parameters is kept small relative to having parameters for each interacting pair. With N different molecule types as possible interaction partners, the number of parameters that could be used if each type of pair was treated separately would vary as $N(N+1)$, but with parameters tied to molecules, the number grows proportional to N. And, of course, the values used in $V_{\text{electrical}}$ are also associated with individual monomers as they are molecular response properties.

The idea behind using a product form of parameters tied to individual molecules is a combining rule. It goes back to 6-12 forms for rare gas potentials [$V(r) = C_6/r^6 + C_{12}/r^{12}$] whereby good quality potentials were obtained for heterodimers, e.g., NeAr, by taking the C_6 and C_{12} parameters to be products of the square roots[4] of the parameters for pure dimers, as in $C_{12[\text{NeAr}]} = (C_{12[\text{NeNe}]})^{1/2}\,(C_{12[\text{ArAr}]})^{1/2}$. A basis for a transferable form via a different combining rule[5,6] has been considered by Thakkar.[7] This combining rule uses C_6 coefficients for a pair of like species, e.g., $C_6^{\text{A-A}}$, and their dipole polarizabilities, α, for a C_6 coefficient for interactions of unlike species.

$$C_6^{\text{A-B}} \cong \frac{2\alpha_{\text{A}}\alpha_{\text{B}} C_6^{\text{A-A}} C_6^{\text{B-B}}}{\alpha_{\text{B}}^{\,2} C_6^{\text{A-A}} + \alpha_{\text{A}}^{\,2} C_6^{\text{B-B}}} \tag{4}$$

Thakkar looked at a sizable number of interactions and found that the combining rule in eq 4 produced a root mean square error of 0.52%[7] relative to the directly evaluated C_6 coefficients of mixed pairs. Though eq 4 looks different from the product form for C_6 coefficients in eq 3, i.e., $c_\alpha c_\beta$, eq 4 does, in fact, reduce to such a product form, $C_6^{\text{A-B}} = (C_6^{\text{A-A}})^{1/2}(C_6^{\text{B-B}})^{1/2}$, under the condition that $C_6^{\text{A-A}}/C_6^{\text{B-B}} = \alpha_{\text{A}}^{\,2}/\alpha_{\text{B}}^{\,2}$. This condition corresponds to a static, or frequency independent, approximation in the relation of C_6 coefficients to the otherwise frequency-dependent dipole polarizabilities. Consequently, going from the use of eq 4 to the corresponding part of eq 3 in a model potential has a physical basis that does not significantly sacrifice accuracy and transferability.

In our investigations, the values for the c and d parameters in eq 3 have been obtained either by using spectroscopic data or by using ab initio calculations of an interaction potential surface. Rotational constants from microwave spectra of homomolecular dimers are especially useful in obtaining c and d parameters for some molecules because the measured values are averages over the dimer's vibrational ground state. The measured values thereby correspond to a sampling of the interaction potential energy surface. For the acetylene dimer, there are experimental rotational constants not only for $(HCCH)_2$[8] but also for a number of deuterated forms.[9] The vibrational ground states of each of the isotopically substituted forms sample the potential surface differently. Thus, the set of isotopic data provides an excellent base for parameter selection, and we used it to find the small set of parameters needed to represent an acetylene molecule via eqs 1−3.[10] Obtaining the parameters required calculational treatment of the vibrational motion in the ground state and a sequence of repeated calculations to search for the best c and d parameters. A comparison of the essential

TABLE 1: Ground Vibrational State Rotational Constants of the Acetylene Dimer

	rotational constant (MHz), $\langle B + C \rangle/2$	
isotopomer	calcd with model potential[10]	spectroscopic[a]
HCCH−HCCH	1855	1856.6
HCCD−HCCH	1852	1854.7
DCCD−HCCH	1762	1760.1
HCCD−HCCD	1814	1815.8
DCCD−DCCH	1776	1778.7
DCCD−DCCD	1689	1688.2

[a] The spectroscopic value for HCCH−HCCH is from ref 8, and the other spectroscopic values are from ref 9.

TABLE 2: Hydrogen, Acetylene and Benzene Model Potential Parameters

	c parameter (au)			*d* parameter (au)		
site[a]	H_2	HCCH	C_6H_6	H_2	HCCH	C_6H_6
H-atoms		0.6	1.8356	151.525	19.0	
C-atoms		10.6			3230.0	1494.721
center of mass	1.651		23.8460	419.03		
outer sites	0.879					39.6467

[a] Relative to centers of mass for the molecules, the H-atom sites in H_2 are at ±0.3715 Å, and the outer sites are at ±0.5715 Å;[2] the H-atom sites in HCCH are at ±1.6637 Å and the C-atom sites are at ±0.6012 Å;[10] and for benzene, the H-atom sites are 2.481 Å from the center, the C-atom sites are 1.397 Å from the center, and the outer sites are 2.726 Å from the center along each C-H bond.[11]

results from the model potential determined in this way and the experimental values is given in Table 1, and the parameter values that were found are included with those given in Table 2.

Instead of spectroscopic values, ab initio calculations can be used for parameter selection. This has been done by obtaining a grid of interaction potential surface points and then, in a least squares sense, adjusting the *c* and *d* parameters to bring the model potential as close to the ab initio surface points as possible. We have done this to obtain representations (i.e., the molecular *c* and *d* parameters) for H_2 via a surface for $(H_2)_2$[2] and then for benzene via a surface for the $H_2-C_6H_6$ dimer.[11] The values obtained are in Table 2. Figure 1 shows a representative comparison of certain slices of the $H_2-C_6H_6$ dimer interaction surface for the model potential versus the ab initio values and also a comparison for another problem treated this way,[12] HCCH−$H(CC)_{2,3}$H. It is important to realize that the quality of the fit in Figure 1a ($H_2-C_6H_6$) was achieved with four nonzero *c* and *d* parameters for benzene because the parameters for H_2 were transferable and had already been determined.[2] At the same time, the use of ab initio data versus spectroscopic values means that lingering sources of error due to incompleteness in the basis set and/or incompleteness in the level of correlation can be transmitted via the fitting to the model potential. The quality attainable, given the concise functional form of the model potential, seems a suitable match for the quality of the information used so far in determining *c* and *d* parameters.

The model potential should be especially appropriate for clusters with interaction strengths between extremely weak dispersion interactions, such as among rare gas atoms, and strong intermolecular interactions that produce substantial changes in the electronic structure of the interacting monomers. Typically, clusters of quadrupolar molecules are in this intermediate range. We note that for interactions involving rare gas atoms, $V_{\text{electrical}} = 0$, and hence, dispersion is a crucial part of the potential. For these types of clusters, the model potential will do no better

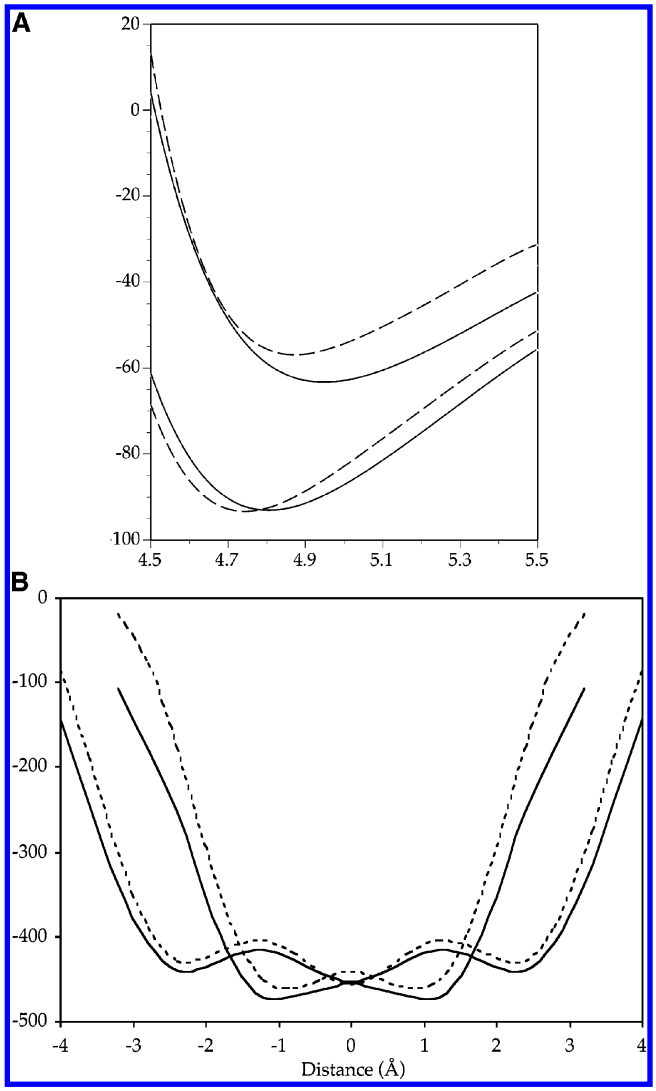

Figure 1. (a) Ab initio potential (solid lines) versus the model potential (broken lines) for the interaction energy (in cm^{-1}) along two slices of the H_2−benzene interaction potential energy surface. Both slices are for arrangements where the center of mass of H_2 is in the plane of benzene and on a line bisecting the angle between adjacent C−H bonds. The horizontal axis gives the distance from the center of mass of benzene to the center of mass of H_2. The slice represented by the upper two curves has the H_2 collinear with the C−H bond whereas the lower slice has the H_2 oriented perpendicular to the benzene plane. Comparisons of other slices have been given elsewhere.[11] (b) Comparison of acetylene−polyyne interaction energies from ab initio calculations (solid lines) and using the model potential (broken lines).[12] The double-well potential is for sliding acetylene along the diacetylene molecule with acetylene's orientation being perpendicular to the polyyne. The interaction curves with three wells are for triacetylene. The strength of the interaction is given in cm^{-1} (vertical axis). The position of the acetylene from the midpoint of each polyyne chain is given in Å on the horizontal axis.

than the best 6-12 potential would do for a pair of rare gas atoms. At the other extreme, for interactions that might be seen as strong—among weak noncovalent interactions—the possibility for electronic structure changes in the monomers and even small geometrical changes limits the use of the model. Although polarization effects are incorporated in the electrical part of the potential, the effect of polarization on dispersion [see, for instance, refs 13−16] and other higher order effects are not. Interestingly, in exploring the very strongly perturbing effects of an approaching H^+ to small molecules, something well beyond weak interaction among neutral species, we have

found[17,18] that the electronic structure changes throughout much of the interaction potential surface, and even the proton-transfer potential for $HCN-H^+-NCH$,[18] follow very much from the polarization and hyperpolarization response of the molecule to the charge of the proton.

For typical sizes of molecular dipoles and quadrupoles, there tends to be a stronger polarization effect on neighboring molecules from a dipolar molecule, for instance HF, than from a quadrupolar molecule such as N_2. This places the problem of interacting quadrupolar species midway between the very weak interactions of rare gas atoms and the strongest of electrical interactions among neutrals. In turn, the back or mutual polarization effects and other higher order effects that go with electronic structure changes of the monomers will tend to be more ignorable for a collection of N_2 molecules than for a collection of HF molecules. Hence, the MMC type of model potential is likely to achieve its maximum accuracy by treating collections of quadrupolar species. Note that the model potential includes three-body (molecule−molecule−molecule) interactions that arise from polarization, and often these seem to be the most important part of nonpairwise interactions among closed-shell, neutral species.

A key physical basis for the modeling scheme that we have been using to understand phenomena of collections of quadrupolar molecules is that of classical, electrical interaction. There are a growing number of model potential schemes that are built on, or that utilize, rigorous and extensive treatment of electrical interaction. In fact, this is emerging rapidly as a powerful new class of computational chemistry tools. To highlight a few that use electrical interaction analysis in extended ways, we first note that Applequist has modeled electrical response between molecules in a very elegant and powerful fashion that provided useful theoretical tools for potential modeling.[19] Buckingham and Fowler used electrical interaction to predict the shapes or preferred structures of weakly attached molecules in one of the earliest model potentials.[20] Ren and Ponder[21,22] have used electrical interaction via atomic multipoles as a noncovalent part of the potentials for water and biomolecular systems. Xantheas and co-workers have developed a model potential using classical electrical polarization for dealing with water clusters and ice.[23] Krimm and co-workers have a sophisticated model potential scheme built on classical electrical interaction and with adjustable parameters chosen on the basis of spectroscopic data.[24−26] Through these and many other schemes for potential modeling, it seems increasingly clear that much can be learned about weak, noncovalent interaction chemistry starting from classical electrical analysis.[27] The details of how far to go with that analysis and how extensive to be in the functional form of the nonelectrical part are still open questions in some sense, but in part, that has to do with there being many different application problems with different needs.

Theoretical and Computational Approach

Certain ab initio and dynamical calculations have been a part of the new results presented here and of our recent investigations on the interactions of small clusters discussed here.[2,10−12] All these ab initio calculations have been carried out at the MP2 level in the treatment of electron correlation. The preferred basis set choice for our calculations is Dunning's aug-cc-pVTZ set,[28] but in some cases smaller basis sets have been employed, such as the cc-pVTZ set. In the ab initio calculations, the monomers are fixed at an equilibrium structure or else at the on-average structure of the ground vibrational state. Counterpoise correction via the Boys−Bernardi scheme[29] is applied for all final energies. Certain of the ab initio MP2 calculations reported here were carried out using the PQS program package.[30] Figures showing molecular structures were generated with Spartan '02.[31]

Vibrational analysis is a very important part of studying weakly bound clusters of all types, not only those of quadrupolar molecules. The zero point energy of the ground vibrational state can set a system's lowest energy substantially upward from the already shallow minimum of a typical weakly bound cluster. One may regard the ZPE as "consuming" stability, and in the case of $(H_2)_2$, around 90% is consumed in that the minimum in the potential surface is -30 cm^{-1} yet the energy of the ground vibrational state is around -3 cm^{-1}.[2] The technique of rigid body diffusion quantum Monte Carlo (RBDQMC)[32,33] is ideal for cluster vibrations and for our model potentials. This is because the computational costs of RBDQMC are in its repeated energy evaluations, and the model potential we employ is especially concise (i.e., computationally inexpensive).[34] The starting point for RBDQMC, Anderson's diffusion quantum Monte Carlo (DQMC) method,[35] is based on an equivalence of the differential equation for diffusion and the time-dependent differential Schrödinger equation on replacing the time variable in the Schrödinger equation by an imaginary time variable. Monte Carlo (MC) techniques for numerical solution of the diffusion equation are then used to simulate the solution of the modified Schrödinger equation via pseudoparticles, or psips,[35] that propagate in randomized, discrete steps in imaginary time. After many time steps, the distribution of psips reflects the ground state. RBDQMC follows from DQMC[35] by having the propagation steps include rotation of a rigid molecule about its principal axes in addition to the usual translation of masses, which are now the molecular centers of mass. An advantage of the rigid body restriction is that for a given precision in the simulation, longer time steps can be used because the high-frequency intramolecular vibrational motions are excluded. Gregory and Clary have shown good agreement of DQMC (without rigidity) and RBDQMC for zero-point energies and rotational constants.[36] For our RBDQMC calculations, the time step is usually around 1.0 au (time) [$=1.0\hbar/E_h = 2.41888 \times 10^{-17}$ s.] The number of DQMC-psips in our calculations is 6000−8000. The energy and property evaluations are performed for at least 100 000 time steps each, and this follows a lengthy equilibration sequence. The RBDQMC simulation yields weights that reflect but are not strictly the same as the vibrational state probability densities.[37] The true probability density may be obtained by descendant weighting,[38,39] and in our calculations, rotational constants such as those in Table 1 have been obtained by averaging the inverses of the principal moments of inertia with these probability densities.

Stabilities and Structures of Small Clusters of Quadrupolar Molecules

The equilibrium structures of dimers of quadrupolar species are often T-shaped because that is the energetically most favorable arrangement of two ideal, point quadrupoles. However, a slipped parallel arrangement (Figure 2) has nearly the same interaction energy and is a generally favorable arrangement, too. $(CO_2)_2$, for example, takes on the slipped parallel form.[41] A T-shaped pair of quadrupole molecules, such as $(HCCH)_2$, will exhibit two T-shaped forms, with the difference being which molecule is the stem and which is the top of the T. If the molecules are the same, then the two T-shaped forms are equivalent, and furthermore, the interconversion pathway can include the slipped parallel form. This is shown in Figure 3 for H_2-H_2, for which the interconversion pathway has a

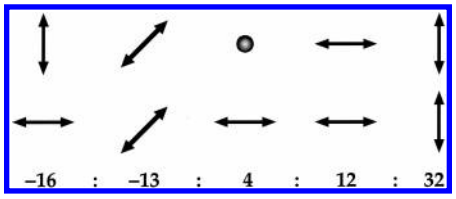

Figure 2. (Adapted from Stone[40]) Illustration representing five particular orientations, left to right, of a pair of ideal quadrupoles with each pair at the same separation distance. The double arrow represents the form of an ideal quadrupole with the ends of like charge and the middle of opposite charge. The middle pair has the top quadrupole perpendicular to the plane of the page. The ratio of the classical, electrostatic interaction energies is given by the values below each pair, starting at the leftmost with the most attractive form (T-shaped), then the slipped parallel form, and then three that are not attractive.

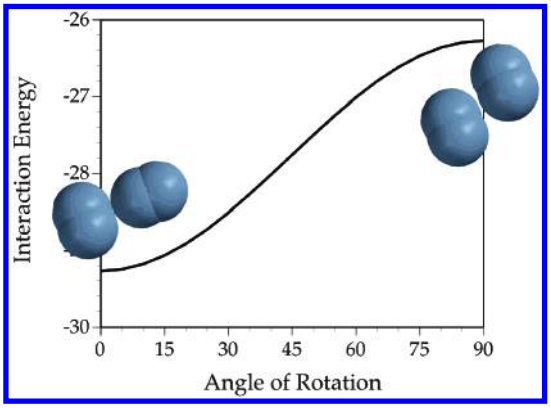

Figure 3. Interconversion potential for the H_2-H_2 dimer.[2] The vertical axis is the interaction energy in cm^{-1} relative to separated monomers. The horizontal axis is an orientation angle for one H_2 molecule in the dimer that takes the structure from the equilibrium T-shaped form (0°) to a slipped parallel form (90°). The 90° structure is a transition state for the interconversion between two equivalent T-shaped structures wherein the base of the T becomes the top of the T and vice versa. The transition state is only 3 cm^{-1} less stable than the equilibrium, and this is partly due to the fact that T-shaped and slipped parallel are energetically preferred arrangements of two quadrupoles as in Figure 2.

slipped parallel arrangement as the saddle point. Partly because this saddle point structure is a favorable orientation for quadrupolar species, the energy barrier of the interconversion is quite small, about 3 cm^{-1}. Although dispersion contributions to the total interaction energy can be relatively sizable, their orientational influence does not tend to overcome the influence of quadrupole−quadrupole interactions.

Stabilities of weakly bound clusters, with stability taken to be positive (the energies of separated monomers less the energy of the cluster at equilibrium), tend to be smaller for clusters of quadrupolar molecules than for clusters of dipolar species. As well, the clusters of quadrupolar species tend to have especially shallow regions of the potential surface and that makes for substantial anharmonicity effects in the weak, or intermolecular, vibrational modes.

Trimers of quadupolar molecules, such as $(H_2)_3$ and $(HCCH)_3$, are quite often cyclic. These structures represent a compromise arrangement away from the preferred T-shaped arrangement between each pair of molecules. The compromise in the arrangements enables the cluster to close the ring so as to have three favorable pair interactions instead of two and to do so without losing much of the T-shaped attraction between each pair. We may think of this as each T-shaped pair distorting along (or nearby) a potential curve, such as the one in Figure 3, to form a three-membered ring. Clearly, the energy to distort is small, and so, for example, we find that the stability of $(H_2)_3$ is

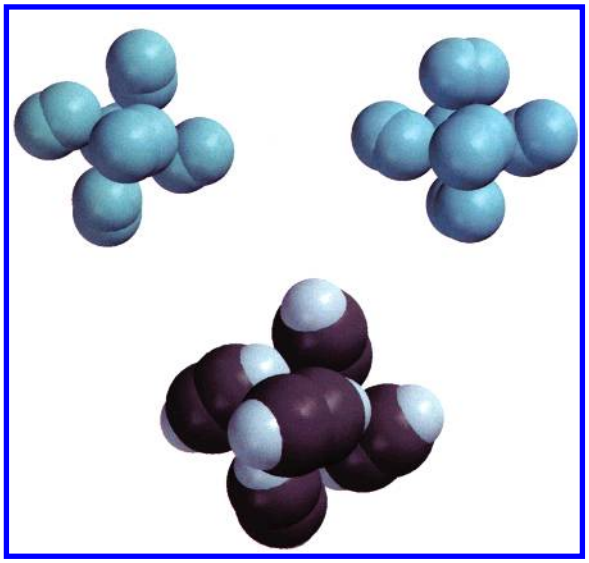

Figure 4. High-symmetry equilibrium structures of $(H_2)_6$ (top) and a similar equilibrium structure of $(HCCH)_6$ (bottom). Each of the structures shows equivalent four-membered puckered cyclic rings in each of three orthogonal planes. As shown for $(H_2)_6$, there are two forms of these six-membered clusters, one with molecules on opposite points from the center being parallel (top left) and one with them being nonparallel (top right). The model calculations show these are very nearly equal in energy, with the top right structure 3 cm^{-1} more stable than the top left structure.

very close to 3 times the stability of the H_2-H_2 stability in the optimum T-shaped arrangement.[2] The model potential gives 29.3 cm^{-1} for $(H_2)_2$, and 3 times that, 87.9 cm^{-1}, is very close to the 86.0 cm^{-1} stability of the cyclic trimer from the model potential. Likewise, from ab initio calculations (MP2/aug-cc-pVTZ), the values are 27.4 cm^{-1} for the stability of the dimer and 83.1 cm^{-1} for the trimer. Also, the interaction energy of $(HCCH)_3$[42] turns out to be similar to 3 times the pair energy of the T-shaped HCCH-dimer. Hence, there tend to be only slight losses in stabilization from distorting each of the T's to make trimers into a cyclic form.

The tetramers of hydrogen and of acetylene, $(H_2)_4$ and $(HCCH)_4$, have a puckered, cyclic form. In this way, there are not only four favorable T-shaped interactions but also two, slightly distorted slipped parallel interactions. Tetramers can be especially good clusters for quadrupolar molecules. The hexamer $(H_2)_6$ is interesting in that the global minimum energy structure has three interconnected, puckered, four-membered cyclic structures in perpendicular planes. Also, there are two energetically similar forms, differing only in an orientation of opposing H_2's (Figure 4). The same thing is found for $(HCCH)_6$. Once again, the small loss in interaction energy from orientational distortion allows for structures that have multiple, favorable pair interactions around one molecule. This is not typical of clusters of dipolar molecules.

Mixed dimers of quadrupolar species often have T-shaped equilibrium structures. Our ab initio calculations have already confirmed this for H_2-HCCH[43] and for $H_2-C_6H_6$,[11] and we have now found this to be true for $HCCH-C_6H_6$ where the equilibrium structure has the acetylene aligned with the benzene C_6 symmetry axis. Trimers and larger clusters of purely quadrupolar molecules will tend to follow the pattern for pure trimers and so on by having minima for cyclic or ring-like forms. However, for mixed species, any differences in sizes and shapes among the molecules will play a role in how the quadrupole-quadrupole interactions combine with other features such as dispersion and close-in repulsion.

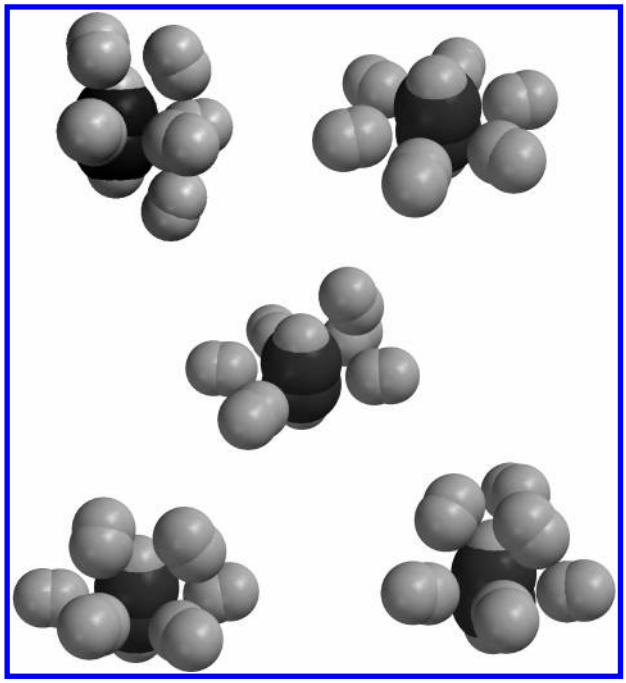

Figure 5. Five lowest energy structures of $(H_2)_6$−HCCH obtained from model potential calculations. The top left structure has a stability of 758 cm^{-1}, whereas the high-symmetry structure (top right)[43] has a stability of 759 cm^{-1}. The middle structure's stability is 761 cm^{-1}, whereas the bottom two structures are at 768 cm^{-1}.

An intriguing example of structures that develop for collections of nondipolar molecules is the pinwheel structure we have found for $(H_2)_6$−HCCH.[43] The preferred structure for the H_2−HCCH dimer is T-shaped with the H_2 as the stem of the T. In the pinwheel structure of $(H_2)_6$−HCCH, each H_2 has the preferred dimer-like position with respect to acetylene because the H_2's encircle the middle of the acetylene molecule 60° apart from one another (Figure 5). The arrangement of adjacent H_2 molecules is somewhat between slipped parallel and T-shaped, and hence, the H_2−H_2 interactions do not significantly work against the stability of the six H_2−HCCH interactions. On the other hand, structures that have three-membered rings of two H_2's and HCCH are also favorable for this particular cluster, and as shown in Figure 5, there are at least five minima of $(H_2)_6$−HCCH that are within a very small range of energies. This range, according to the model potential, is only 10 cm^{-1}, and this highlights a unique surface feature wherein distinctly different minima have essentially the same energy. There is substantial freedom, from the standpoint of potential energy, for vibrational excursions that would include many of these structures rather than allowing only for small excursions from one particular structure.

Intermediate to solid-phase structures and dimers and trimers are large clusters that begin to show some of the packing arrangements of the solid or solid phases, and for quadrupolar species, it is interesting to understand how small cluster behavior evolves into the interactions that determine the structure of crystalline forms of a substance. We have carried out calculations of this sort for H_2 clusters[2] and acetylene clusters,[42] and it is clear that much more can be learned via calculations using realistic model potentials. In the case of pure acetylene, there are two solid phases,[44−47] cubic and orthorhombic, and both exhibit T-shaped pairs of monomers. At a temperature of 133 K, there is a first-order phase transition between the high temperature cubic phase and the orthorhombic phase. We have applied our interaction model to fairly large clusters in arrangements corresponding to both solid phases. These structures with finite numbers of molecules were constructed by surrounding a central molecule with acetylenes in successive shells, maintaining the symmetry of the given crystalline form. Within the symmetry constraints of either a cubic or orthorhombic crystal, structural parameters for clusters with 79, 201 and 391 acetylenes were optimized. There was rapid convergence of these structural parameters with respect to increasing cluster size. On extrapolation to an infinite number of molecules, the model potential results place both forms very close in energy, within 3 kcal mol^{-1} of each other.[42] Calculations with the model potential to find the optimum structure of $(HCCH)_{13}$ showed that this cluster resembles the cubic crystal, not the orthorhombic structure. However, with fewer than 13 monomers, there are noticeable differences from the cubic crystal form, though certain of these differences involve distortions along flat directions on the potential surface. For instance, though the structure of $(HCCH)_6$ (Figure 4) may not reveal itself as being like the cubic crystalline form, the difference follows from its potential surface being shallow with respect to the twisting of opposite molecules.[42] Hence, with increasing size, the small clusters rather quickly take on structural characteristics of the infinite crystal, and importantly, of the cubic not orthorhombic form. An argument for this difference is that there are six T-pairings per monomer in the cubic form but only four in the orthorhombic form.[42]

TABLE 3: Stabilities (cm^{-1}) of Pure and Mixed Hydrogen and Acetylene Clusters

cluster	ref	stability at equilibrium[a]	stability with weak mode ZPE[b]
$(H_2)_2$	2	29.6	0.6
$(HD)_2$		29.6	1.4
$(D2)_2$		29.6	2.7
$(H_2)_3$	2	86.0	2.1
$(H_2)_4$	2	145	4.8
$(H_2)_6$	2	292	12
$(HCCH)_2$	10	503	372
$(DCCD)_2$	10	503	386
$(HCCH)_3$	42	1513	1151
$(HCCH)_4$	42	2360	1827
H_2−HCCH	43	124	12
$(H_2)_2$−HCCH	43	253	25

[a] The stability at equilibrium is the energy of the separated monomers less the energy of the cluster at its equilibrium structure. [b] The stability with weak mode zero point energy is the energy of the separated monomers less the energy of the cluster in its ground vibrational state treating the monomers as rigid.

Unique Features of Potential Surfaces of Clusters of Quadrupolar Molecules

In several of our studies of clusters of quadrupolar molecules, unique potential surface features and associated phenomena have been revealed. Primarily, these features develop for quadrupolar more so than for dipolar species because the quadrupolar interactions allow for greater distortions. The first feature of note is that the shallowness of the surfaces goes along with substantial zero point vibrational energies. As already mentioned, the ZPE can consume a large fraction of the well depth. Table 3 gives values for the stabilities of a number of small clusters containing hydrogen and acetylene molecules, both equilibrium stabilities (well-depths) and stabilities with weak mode ZPE correction. These were obtained by RBDQMC calculations using our model potential.

Another interesting feature of the potential surfaces of interacting quadrupolar species is something that can be regarded

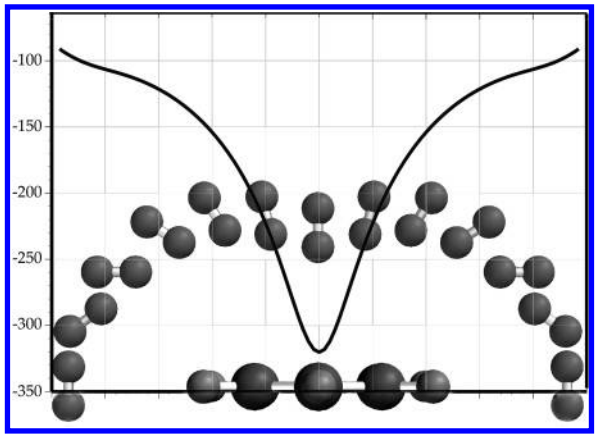

Figure 6. Curve showing the energy calculated from the model potential following the minimum energy path for the $H_2-C_6H_6$ cluster as the H_2 moves from being at the edge and in the plane of benzene to its global minimum energy position along the C6 symmetry axis of benzene. The position of H_2 with respect to benzene at selected points along the minimum energy path is shown by the molecular diagrams. The vertical axis is in cm^{-1} and the horizontal axis gives the distance of the center of mass of H_2 from the benzene C6 symmetry axis. The left and right edges of the graph are 5 Å from the symmetry axis, and the molecule diagrams of H_2 and benzene and drawn to this distance scale. The global minimum has H_2 aligned with the C6 symmetry axis, and there are equivalent structures above and below the benzene ring.

as molecular slipperiness. This is a weak attraction between two molecules that leads to a global minimum energy point that lies within an extended, nearly flat trough. The system is slippery in that one molecule can move along the trough with little change in potential energy. We have found this slipperiness for acetylene interacting with polyynes,[12] and we have found that the polyynes can be capped with simple functional groups[48] so as to make for a trough, running the length of the polyyne, but closed on the ends.

In a large cluster of a hundred or more hydrogen molecules, the unique interaction surface features of quadrupolar molecules along with the size and shape of H_2 yield an interesting feature. Whereas rotating one molecule about its mass center in the middle of a large regular aggregation has a barrier of 60 cm^{-1}, if the orientations of the surrounding shell of 12 hydrogen molecules can change in a concerted way with the internal rotation of the central H_2, the barrier is reduced to less than 1 cm^{-1}.[2] Hence, there is essentially free rotation of the monomers in gas-phase H_2-H_2 (Figure 2)[49,50] and, in a more complicated way, also in H_2-solid, where free internal rotation effects have been recognized.[51]

The interaction of benzene and H_2 is especially interesting for the types of surface features and the likely dynamical behavior that goes with them. Interesting calculational results for the rotational transitions of H_2 weakly attached to benzene have been reported by Hamel and Côté.[52] The surface for $H_2-C_6H_6$ has a minimum with the H_2 along and aligned with the C_6 symmetry axis of benzene. There are two such locations, one on each side of the benzene ring. As shown by the potential energy curve in Figure 6, there is a barrier along the edge of the ring for interconversion from top- to bottom-side attachment. In other words, an H_2 approaching benzene from any direction will find a potential that is smoothly downhill to either axial site. However, once the site is filled, other binding sites develop.[11] In fact, the benzene molecule becomes completely enclosed by a regular arrangement of 20 H_2 molecules in specific sites, as shown in Figure 7.

The sites for H_2 molecules weakly attached to benzene can be categorized as axial (A), above the plane of benzene (B), or along the edge (C). There are six B sites on each face of benzene and there are six C sites along the edge. With the two A sites, this makes for the 20 sites shown for the cluster structure in Figure 7. With fewer H_2 molecules, there are numerous structures for clustering around a benzene molecule,[11] and these have been examined and a pattern has been recognized. It is important that molecules in the B sites, or what we may consider a B ring around the C_6 symmetry axis, can move with small barriers from one B site to another one that is otherwise unoccupied. There is considerable dynamical freedom for B site molecules, even with ground state vibrational energy (see Table 4). There likely exist internal rotor states for certain sized clusters wherein one to six H_2 molecules rotate around the benzene C_6 symmetry axis in the B ring. This is a very special

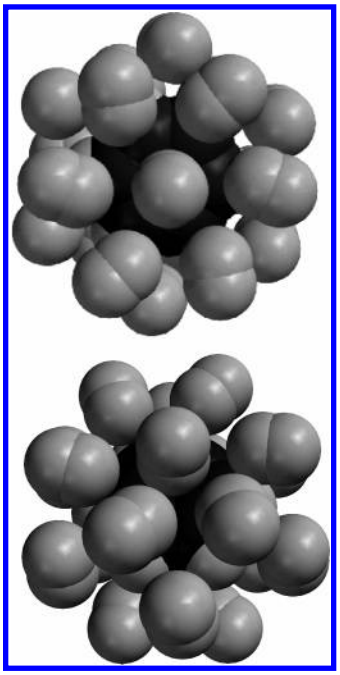

Figure 7. Two views of the low energy structure of the cluster $(H_2)_{20}-C_6H_6$ showing the very regular arrangement of hydrogen molecules enclosing the benzene, as yielded[11] by model potential calculations.The first is with the benzene plane parallel to the plane of the page, whereas the lower view has the cluster rotated, relative to the top view, so that the benzene C6 symmetry axis is pointing upward instead of straight out from the plane of the page. For clustering of H_2 around benzene, the calculations show that along with the two preferred sites where an H_2 is collinear with the benzene C6 symmetry axis, one H_2 above and one below the plane of benzene, six H_2 molecules offset from the C6 axis form a ring above the benzene plane, with a like ring below. Both views show the seven H_2 molecules above the plane of benzene. There is a third ring of six H_2's around the edge of the benzene and these are oriented perpendicular to the plane of the benzene, mostly to have a favorable orientation with respect to hydrogen molecules in the rings above and below the benzene plane.

TABLE 4: Calculated Stabilities (cm^{-1}) of $(H_2)_n-C_6H_6$ Clusters

cluster	stability at equilibrium[a]	stability with weak mode ZPE[b]
$H_2-C_6H_6$	320	110
$(H_2)_2-C_6H_6$	643	222
$(H_2)_3-C_6H_6$	782	266
$(H_2)_4-C_6H_6$	927	306

[a] The stability at equilibrium is the energy of the separated monomers less the energy of the cluster at its equilibrium structure. [b] The stability with weak mode zero point energy is the energy of the separated monomers less the energy of the cluster in its ground vibrational state treating the monomers as rigid.

kind of potential surface slipperiness, and again, slipperiness seems a unique or maybe prominent feature for interacting quadrupolar species.

Related Quadrupolar Charge Field Interactions

The interaction potential energy surface features for collections of quadrupolar species clearly and consistently show extended regions of flatness and multiple minima—multiple minima energetically close to the global minimum. In the extreme, there are cases of very extended troughs and rings where the surface is essentially flat. And there is almost always softness for orientational distortion away from a minimum energy structure. Though our studies have focused on simple, quadrupolar molecules, there are like consequences of the quadrupolar charge fields when one interacting partner is dipolar. The water−benzene dimer shows a very flat surface for water to "slide" across the face of benzene with an O−H bond directed toward the benzene ring,[53] and there is nearly free internal rotation of the attached water, something that makes for a highly intricate rotational spectrum.[54] Substitution on the benzene ring to yield styrene means a small dipole exists, but the local field around the ring is not significantly changed. Preliminary calculations show comparable slipperiness for water moving across the face of the styrene phenyl group. These surface features will have a dynamical influence because they allow for extensive excursions away from minimum energy structures.

Polyacetylene and polystyrene are among many complicated species with local quadrupolar regions. There is potential technological value in more detailed understanding of dipolar and quadrupolar interactions with locally quadrupolar species. For instance, in the industrial expansion of polystyrene, a volatile blowing agent such as an aliphatic hydrocarbon or chloro-fluoro-carbon is vaporized to expand the foam. Not only are common blowing agents flammable with a high explosion hazard, but also there are detrimental changes to mechanical and other properties of polymers from certain penetrant molecules [e.g., refs 55−57]. There are innovative alternatives, including carbon dioxide,[58,59] supercritical CO_2,[60] argon,[61] and molecular nitrogen.[62] For these nonpolar species, the dependence of the bulk properties of the expanded foam to the interactions of the blowing agent is not established. Hence, representing, modeling and simulating interacting quadrupolar species appears as an important challenge for the technology of certain materials and energy problems.

Finally, we note that the softness and the slipperiness found for interacting quadrupolar species, along with the typical existence of numerous minima mean that small external influences can have important structural and dynamic effects. In particular, an electric field gradient would act directly with local quadrupoles, and thus, some control or direction of cluster growth and formation seems possible. It will be interesting to pursue electrical field and field gradient effects to determine the specific kind of structural influence that can be applied externally under the variety of conditions where cluster interactions of quadrupolar species are at work, including condensed phases.

Conclusions

Quadrupolar charge fields, whether for small molecules, or fragments of large molecules, give rise to very interesting and somewhat unexpected features in weak interaction potential surfaces, especially for collections of several molecules. (1) Even the smallest clusters tend to have numerous binding sites (multiple minima). In part, this develops from the energetic similarity of T-shaped and slipped parallel arrangements of two ideal quadrupoles. (2) The interaction potential surfaces tend to have extended regions of flatness that allow for especially wide-amplitude vibrational excursions. (3) Aggregation of quadrupolar species tends to show different, but energetically competitive, packing arrangements, at least for small assemblies. (4) Because of the relative softness in their interaction potentials, especially with respect to orientational changes, small perturbations (fields, conformational changes, other nearby molecules, atoms, and ions) are likely to have sharper effects for clusters of quadrupolar molecules than for clusters of dipolar molecules. Some other features may not yet have been recognized, but model potentials that allow for the study of large clusters will be increasingly beneficial, especially for understanding the complexities of mixed systems. For instance, applying our model potential to a cluster of benzene and acetylene with six H_2 molecules, we find (Figure 8) that the pinwheel structure of $HCCH-(H_2)_6$ is largely preserved as one end of acetylene finds the optimum weak attachment point on benzene, along the C_6 symmetry axis. This is suggestive of the possibility of quadrupolar liquids, perhaps liquid nitrogen, being used to form a solvent cage that facilitates spectroscopic investigation of clusters such as $HCCH-C_6H_6$ by limiting the vibrational excursions that might take place in the gas phase.

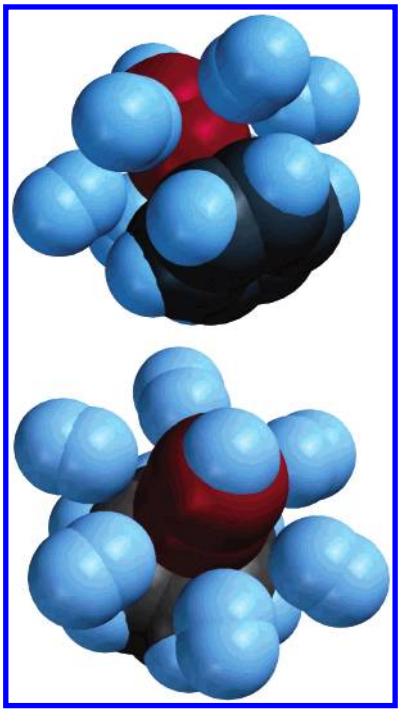

Figure 8. Two views of an equilibrium structure found from model calculations for the cluster $C_6H_6-HCCH-(H_2)_6$. The carbons of the acetylene molecule have been reddened to distinguish acetylene from the benzene ring below.

It is clear that potential modeling for weak interactions of all types requires a certain amount of translating molecular properties into surface features and then into dynamical effects, and these remain open issues as evidenced by the increasing variations in this class of modeling. These should be important issues for biomolecular and materials simulations in that the chemical insight for structures and preferred arrangements of noncovalently interacting, dipolar molecules is not well-matched for quadrupolar species. Potentials used in large-scale dynamical simulations need to be faithful to interactions that produce slippery surfaces, pinwheels, and so on—features that can be evaluated fully in small molecule systems where crucial effects can be unmasked from other effects.

Acknowledgment. This work was supported, in part, by a grant from the Physical Chemistry Program of the National Science Foundation (CHE-0131932).

References and Notes

(1) Buckingham, A. D. *Adv. Chem. Phys.* **1967**, *12*, 107.
(2) Carmichael, M.; Chenoweth, K.; Dykstra, C. E. *J. Phys. Chem. A* **2004**, *108*, 3143.
(3) Dykstra, C. E. *J. Am. Chem. Soc.* **1989**, *111*, 6168; *Chem. Rev.* **1993**, *93*, 2339.
(4) Smith, F. T. *Phys. Rev. A* **1972**, *5*, 1708.
(5) Tang, K. T. *Phys. Rev.* **1969**, *177*, 108.
(6) Kutzelnigg, W.; Maeder, F. *Chem. Phys.* **1978**, *35*, 397.
(7) Thakkar, A. J. *J. Chem. Phys.* **1984**, *81*, 1919.
(8) Fraser, G. T.; Suenram, R. D.; Lovas, F. J.; Pine, A. S.; Hougen, J. T.; Lafferty, W. J.; Muenter, J. S. *J. Chem. Phys.* **1988**, *89*, 6028.
(9) Matsumura, K.; Lovas, F. J.; Suenram, R. D. *J. Mol. Spectrosc.* **1991**, *150*, 576.
(10) Shuler, K.; Dykstra, C. E. *J. Phys. Chem. A* **2000**, *104*, 4562.
(11) Swenson, D. W. H.; Jaeger, H. M.; Dykstra, C. E. *Chem. Phys.*, in press.
(12) Chenoweth, K.; Dykstra, C. E. *J. Phys. Chem. A* **2002**, *106*, 8117.
(13) Jeziorski, B.; Moszynski, R.; Szalewicz, K. *Chem. Rev.* **1994**, *94*, 1887.
(14) Chalasinski, G. *Chem. Rev.* **1994**, *94*, 1723.
(15) Szalewicz, K.; Bukowski, R.; Jeziorski, B. In *Theory and Applications of Computational Chemistry. The First Forty Years*; Dykstra, C. E., Frenking, G., Kim, K. S., Scuseria, G. E., Eds.; Elsevier: Amsterdam, 2005; pp 919−993.
(16) Wormer, P. E. S.; van der Avoird, A. In *Theory and Applications of Computational Chemistry. The First Forty Years*; Dykstra, C. E., Frenking, G., Kim, K. S., Scuseria, G. E., Eds.; Elsevier: Amsterdam, 2005; pp 1047−1077).
(17) Dykstra, C. E. *J. Phys. Chem. A* **2003**, *197*, 4196.
(18) Dykstra, C. E. *J. Mol. Structure (THEOCHEM)* **2004**, *683*, 147.
(19) Applequist, J. *J. Math. Phys.* **1983**, *24*, 736; *Chem. Phys.* **1984**, *85*, 279; *J. Chem. Phys.* **1985**, *83*, 809.
(20) Buckingham, A. D.; Fowler, P. W. *Can. J. Chem.* **1985**, *63*, 2018.
(21) Ren, P.; Ponder, J. W. *J. Comput. Chem.* **2002**, *23*, 1497.
(22) Ren, P.; Ponder, J. W. *J. Phys. Chem. B* **2003**, *107*, 5933.
(23) Batista, E. R.; Xantheas, S. S.; Jonsson, H. *J. Chem. Phys.* **1998**, *109*, 4546; *J. Chem. Phys.* **1999**, *111*, 6011; *J. Chem. Phys.* **2000**, *112*, 3285.
(24) Mannfors, B.; Palmo, K.; Krimm, S. *J. Mol. Struct.* **2000**, *556*, 1.
(25) Palmo, K.; Mannfors, B.; Krimm, S. *Chem. Phys. Lett.* **2003**, *369*, 367.
(26) Palmo, K.; Mannfors, B.; Mirkin, N. G.; Krimm, S. *Biopolymers* **2003**, *68*, 383.
(27) Dykstra, C. E. *Adv. Chem. Phys.* **2003**, *126*, 1.
(28) Dunning, T. H. *J. Chem. Phys.* **1989**, *90*, 1007.
(29) Boys, S. F.; Bernardi, F. *Mol. Phys.* **1970**, *19*, 553.
(30) PQS Version 2.4, Parallel Quantum Solutions, 2013 Green Acres Road, Fayetteville, AR 72703.
(31) Spartan '02, Wave function Inc., Irvine, CA.
(32) Buch, V. *J. Chem. Phys.* **1992**, *97*, 726.
(33) Franken, K. A.; Dykstra, C. E. *J. Chem. Phys.* **1994**, *100*, 2865; *Chem. Phys. Lett.* **1994**, *220*, 161.
(34) Dykstra, C. E.; Van Voorhis, T. A. *J. Comput. Chem.* **1997**, *18*, 702.
(35) Anderson, J. B. *J. Chem. Phys.* **1975**, *63*, 1499.
(36) Gregory, J. K.; Clary, D. C. *Chem. Phys. Lett.* **1994**, *228*, 547.
(37) Reynolds, P. J. *J. Chem. Phys.* **1990**, *92*, 2118.
(38) Coker, D. F.; Watts, R. O. *J. Phys. Chem.* **1987**, *91*, 2513.
(39) Kalos, M. H. *Phys. Rev. A* **1970**, *2*, 250.
(40) Stone, A. J. *The Theory of Intermolecular Forces*; Oxford University Press Press: Oxford, 1996.
(41) Jucks, K. W.; Huang, Z. S.; Dayton, D.; Miller, R. E.; Lafferty, W. J. *J. Chem. Phys.* **1987**, *86*, 4341.
(42) Shuler, K.; Dykstra, C. E. *J. Phys. Chem. A* **2000**, *104*, 11522.
(43) Chenoweth, K.; Dykstra, C. E. *Chem. Phys. Lett.* **2004**, *400*, 153.
(44) Sugawara, T.; Kanda, E. *Science Rept. Res. Inst., Tohoku University Ser. A* **1952**, *4*, 607.
(45) Koski, H. K.; Sandor, E. *Acta Crystallogr. B* **1975**, *31*, 350; Koski, H. K. *Acta Crystallogr. B* **1975**, 31, 933; *Cryst. Struct. Commun.* **1975**, *4*, 343; *Cryst. Struct. Commun.* **1975**, *4*, 337; *Z. Naturforsch.* **1975**, *30a*, 1028.
(46) van Nes, G. J. H.; van Bolhuis, F. *Acta Crystallogr. B* **1979**, *35*, 2580.
(47) McMullan, R. K.; Kvick, A.; Popelier, P. *Acta Crystallogr. B* **1992**, *48*, 726.
(48) Chenoweth, K.; Dykstra, C. E. *Chem. Phys. Lett.* **2005**, *402*, 329.
(49) McKellar, A. R. W. *Astrophys. J.* **1988**, *326*, L75.
(50) McKellar, A. R. W.; Schaefer, J. *J. Chem. Phys.* **1991**, *95*, 3081.
(51) Silvera, I. F. *Rev. Modern Phys.* **1980**, *52*, 393.
(52) Hamel, S.; Côté, M. *J. Chem. Phys.* **2004**, *121*, 12618.
(53) Augspurger, J. D.; Dykstra, C. E.; Zwier, T. S. *J. Phys. Chem.* **1992**, *96*, 7252.
(54) Emilsson, T.; Gutowsky, H. S.; de Oliveira, G.; Dykstra, C. E. *J. Chem. Phys.* **2000**, *112*, 1287.
(55) Zhang, D.; Ward, R. S.; Shen, Y. R.; Somorjai, G. A. *J. Phys Chem. B* **1997**, *101*, 9060.
(56) Gambogi, J. E.; Blum, F. D. *Mater. Sci. Eng. A* **1993**, *162*, 249.
(57) Jabarin, S. A.; Lofgren, E. A. *Polym. Eng. Sci.* **1986**, *26*, 620.
(58) Otake, K.; Webber, S. E.; Munk, P.; Johnston, K. P. *Langmuir* **1997**, *13*, 3047.
(59) Park, C. B.; Behravesh, A. H.; Venter, R. D. *Polym. Eng. Sci.* **1998**, *38*, 1812.
(60) Arora, K. A.; Lesser, A. J.; McCarthy, T. J. *Macromolecules* **1998**, *31*, 4614; *Polym. Eng. Sci.* **1998**, *38*, 2055.
(61) Jacob, C.; Dey, S. K. *J. Cell. Plast.* **1985**, *31*, 38l.
(62) Kumar, V.; Suh, N. P. *Polym. Eng. Sci.* **1990**, *30*, 1323.